Controlling flow turbulence

Shuguang Guan and Y. C. Zhou
Department of Computational Science, National University of Singapore, Singapore 117543, Singapore

G. W. Wei
Department of Computational Science, National University of Singapore, Singapore 117543, Singapore and Department of Mathematics, Michigan State University, East Lansing, Michigan 48824

C.-H. Lai
Department of Physics, National University of Singapore, Singapore 117543, Singapore

(Received 13 September 2002; accepted 13 November 2002; published 17 January 2003)

This paper investigates the viability and effectiveness of using a technique developed for low-dimensional chaotic systems to control flow turbulence governed by the Navier–Stokes equations. By using a global pinning coupling strategy, we show that turbulence can be controlled to desirable time-varying target states, including a spatially extended periodic state and a turbulent one. Exponential convergence to the target state is found and the exponential rate scales linearly to the coupling strength. The linear scaling law breaks down when localized pinning control is applied. A wavelet multiscale technique is utilized for the characterization of both the effectiveness of the present control strategy and the inverse energy transfer in two-dimensional turbulence. © *2003 American Institute of Physics.* [DOI: 10.1063/1.1539017]

Since the pioneer work of Ott, Grebogi, and Yorke in 1990, controlling chaos has been extensively investigated. A variety of approaches, such as the OGY scheme, open-loop strategy, feedback technique and adaptive method, have been developed for the purpose of chaos control. Most early work deals with low-dimensional chaotic systems such as the logistic map and the Lorenz system. Recently chaos control has been gradually carried out in spatially extended dynamical systems, such as coupled map lattices and partial differential equations. These works are motivated by potential applications in laser and plasma physics, chemical reactions, electric circuits, neuronal networks as well as secure communication. One of the most complicated spatiotemporal systems is the real-world fluid turbulence. However, the possibility of controlling flow turbulence by using the control strategies developed in the low-dimensional chaotic system has not been studied. In this paper, we show that the flow turbulence governed by the Navier–Stokes equations can be effectively controlled by global and local pinning methods.

I. INTRODUCTION

Turbulence is abundant and omnipresent in nature.[1] The fascinating complexity of flow turbulence has attracted the attention of philosophers, poets and scientists alike for centuries. Turbulence is advantageous in many circumstances, such as fuel mixing in engine and heat dispersion in atmosphere, but is undesirable in many other cases, such as aircraft safety. The control of turbulence is thus of great interest and importance. Although the engineering perspective of turbulence control has been studied over decades in terms of passive and active control,[2] theoretical understanding from the point of view of nonlinear dynamical systems and controlling chaos has been rarely addressed.

A variety of techniques have been proposed for controlling complex dynamical systems[3] since the first work by Ott, Grebogi, and Yorke (OGY).[4] The basic idea of OGY is to take advantage of the sensitivity to small disturbances of chaotic systems to stabilize the system in a desirable unstable periodic orbit naturally embedded in the chaotic attractor. While detailed system equations are not required for the control, a learning process is necessary to obtain the essential information required for the control, such as the location and the eigenvalues of the desirable unstable periodic orbit in the phase space. Nevertheless, it is generally difficult to apply the OGY idea to high-dimensional systems, such as the turbulence to be addressed in the present work, although for certain situations, for example, in turbulent boundary layers, a low-dimensional dynamical system model can be set up.[5] A more practical method proposed by Pyragas[6] utilizes a time-delayed feedback to some dynamical variables of the system. A periodic orbit embedded in the chaotic set can be stabilized when its period matches the delay time. Moreover, control of spatiotemporal chaos was reported for the one-dimensional complex Ginzburg–Landau equation (CGLE).[7] Suppression of spurious oscillations in spatiotemporal systems was studied and an angular momentum injection technique was proposed for taming the wake turbulence behind a bluff body.[8] However, the viability and effectiveness of using the techniques developed for low-dimensional chaotic systems over the past 10 years for controlling true flow turbulence described by the incompressible Navier–Stokes equations have not been exploited yet, though the control of chaos, especially spatiotemporal chaos, was partially motivated by the goal of controlling fluid turbulence. The purpose of this work is to investigate the control of flow turbulence

by using chaos control strategies. It is emphasized that true flow turbulence governed by the incompressible Navier–Stokes equations differs fundamentally from the ''amplitude/defeat turbulence'' and the ''phase turbulence'' within the spatiotemporal chaos regime governed by the complex Ginzburg–Landau equation. First of all, the complex Ginzburg–Landau equation is an amplitude equation, and it describes the dynamics near the Hopf bifurcation in spatially extended systems. In contrast, the incompressible Navier–Stokes equations have a vector equation and a coupled scalar equation and they describe real hydrodynamic flows. Second, the complex Ginzburg–Landau equation is a prototype of spatiotemporal chaos, which might be regarded as a population of chaotic oscillators locally coupled by diffusion. Its transition from stationary states to unsteady states has been studied in terms of Benjamin–Feir instability and the Eckhaus instability, with detailed phase diagram having been identified. Nevertheless, for the Navier–Stokes equations, the transition from laminar flow to turbulence remains a long-lasting open question for many real-world systems. Finally, solving the incompressible Navier–Stokes equations is a very technical issue due to the ill-posedness in their boundary conditions. Many available computational schemes have their limitations. Completely different conclusions might be obtained if an inappropriate solution method or control scheme is utilized. Therefore, the current investigation is not just a simple application of existing techniques.

In the following section, the dynamical model and the numerical method are described. In Sec. III, we show that the flow turbulence can be controlled to different targets, such as a periodic pattern or another turbulent state by using either global pinning coupling or local pinning coupling. A wavelet method is used to characterize the effectiveness of the control strategy and the energy transfer in two-dimensional turbulence in Sec. IV. This paper ends with conclusional remarks.

II. THE MODEL AND NUMERICAL SOLUTION

Flow turbulence is characterized by both the coexistence of a variety of scales and the energy transfer among the scales due to the nonlinear interactions. In three-dimensional turbulence, the energy transfer among different scales of motion is mainly through the vortex stretching process, which essentially is a three-dimensional mechanism and can never occur in two-dimensional flow.[9] However, in the past several decades there is an increasing interest to investigate the behavior of two-dimensional incompressible Navier–Stokes equations in terms of two-dimensional turbulence. Nowadays, it is believed that the theoretical study of two-dimensional turbulence is one of the key approaches for the understanding of flow turbulence and is of fundamental importance in geophysics, meteorology, and magnetohydrodynamics.[10] Furthermore, two-dimensional turbulence is shown to exhibit characteristics that differs fundamentally from its three-dimensional counterpart.[11] In the framework of direct numerical simulation (DNS), we consider the two-dimensional incompressible Navier–Stokes equations

$$\frac{\partial \mathbf{u}}{\partial t}+\mathbf{u}\cdot\nabla\mathbf{u}=-\nabla p+\frac{1}{\mathrm{Re}}\nabla^2\mathbf{u}, \qquad (1)$$

$$\nabla\cdot\mathbf{u}=0,$$

where p is the pressure, Re is the Reynolds number and $\mathbf{u}=(u,v)$ is the velocity field vector which has its x and y component $u(x,y,t)$ and $v(x,y,t)$, respectively. The flow is bounded in a square domain $[0,2\pi]\times[0,2\pi]$ with the periodic boundary condition in each direction. To solve the incompressible Navier–Stokes equations within the turbulence regime, the choice of an appropriate numerical scheme is of particular importance due to the lack of a governing equation for the pressure field, while the velocity fields are over determined. In the present work, the Fourier pseudospectral method is implemented for the space discretization, and the Adams–Bashforth–Crank–Nicolson (ABCN) scheme is used for the time discretization. The above numerical scheme ensures divergence-free velocity fields and has the spectral precision for the space discretization and the second order precision for time integration. Its validity has been extensively tested.[12] In the numerical integration, the time increment Δt is chosen to be 0.0025 and 256 grid points are used in each direction ($N_x=N_y=256$). All the numerical results have been confirmed by setting different grids and time step.

For DNS of freely decaying two-dimensional turbulence, initial conditions affect the time evolution of the turbulent field. Usually they are given in Fourier (wave number) space by a zero-mean Gaussian random field with random phases. The variance of the initial spectrum can be chosen to approximately satisfy the energy spectrum of the desired form[13]

$$E(k,0)\sim ke^{-(k/k_0)^2}, \qquad (2)$$

or

$$E(k,0)\sim k^4e^{-(k/k_0)^2}. \qquad (3)$$

Here k_0 is a constant and it can be adjusted to make the energy peak at a desired wave number. For Eq. (2), the energy peak is at wave number $k_0/\sqrt{2}$, while for Eq. (3) it is $\sqrt{2}k_0$. Therefore, the second form distributes more energy at large wave numbers. In our study, for the fluid system to be controlled (response system), the initial conditions are taken to satisfy Eq. (2) with $k_0=5.0$. The dynamics of Eq. (1) is set to a turbulent regime by taking $\mathrm{Re}=5000$.

III. THE CONTROL OF TURBULENCE

In the rest of this paper, we consider two important examples of controlling two-dimensional turbulence. In the first example, we study the viability and effectiveness of controlling a turbulent state into the time-varying analytical solution of the Navier–Stokes equation[12]

$$u_t(x,y,t)=-\gamma\cos(kx)\sin(ky)e^{-2k^2t/\mathrm{Re}},$$
$$v_t(x,y,t)=\gamma\sin(kx)\cos(ky)e^{-2k^2t/\mathrm{Re}}, \qquad (4)$$

where k is the wave number taking an integer value, and γ is a constant which is chosen as 0.05 in this study. In the sec-

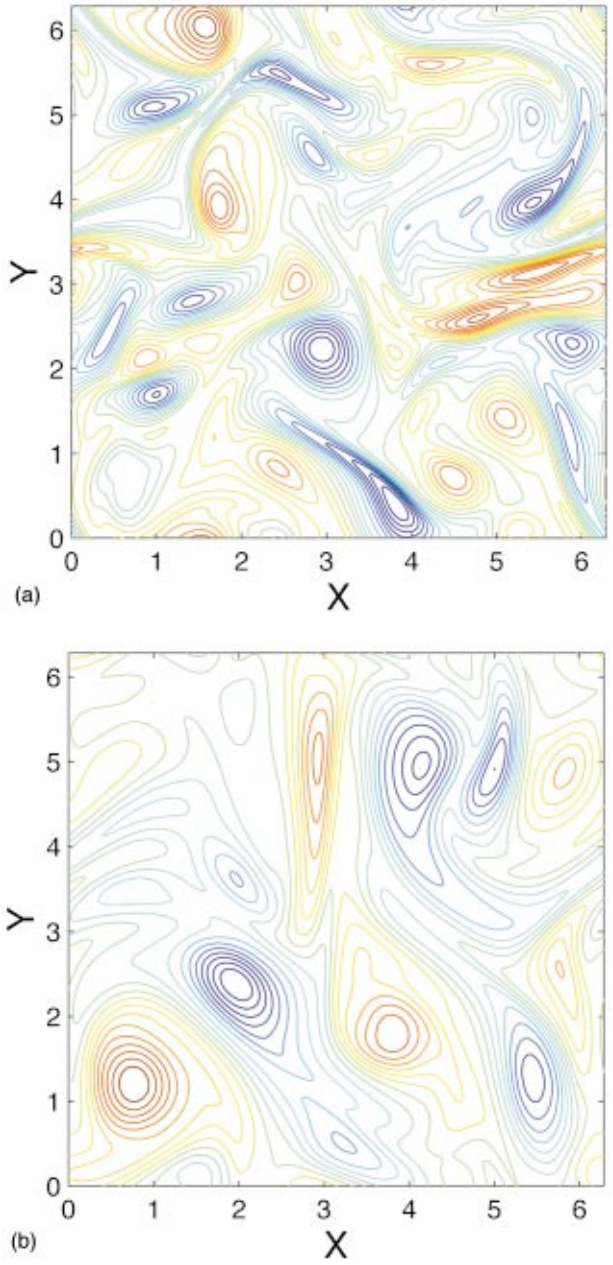

FIG. 1. (Color) Contour plots of the vorticity field of the flow system to be controlled at (a) $t=100$, (b) $t=250$, respectively.

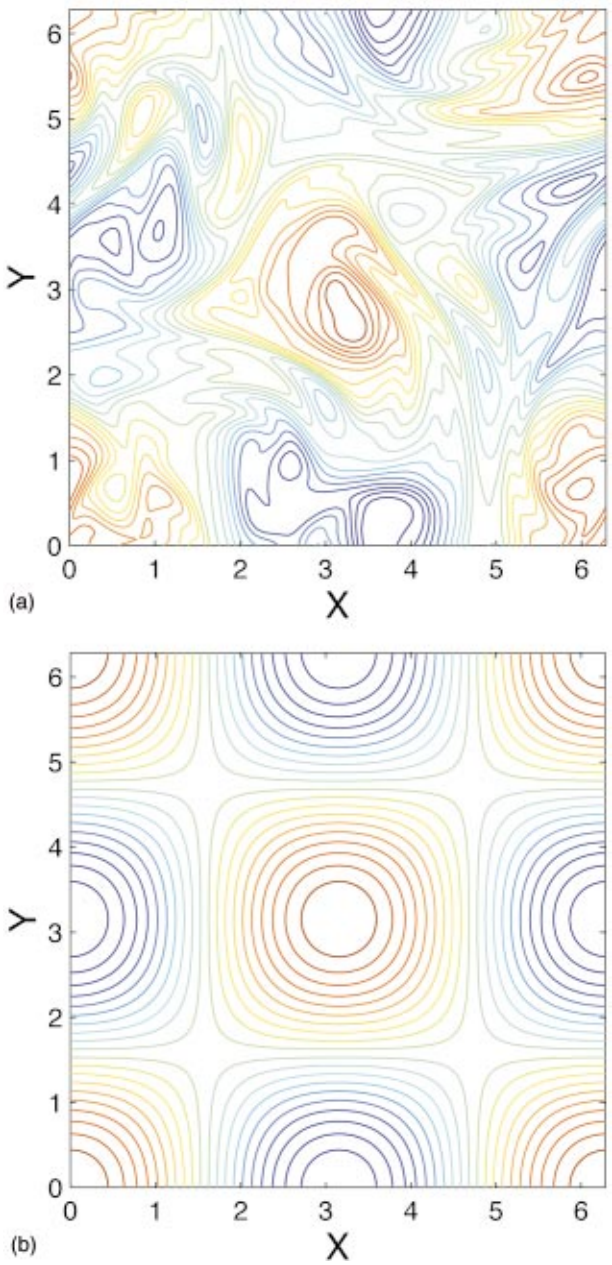

FIG. 2. (Color) Contour plots of the vorticity field of the response system under the pinning control ($\epsilon=-0.1$) at (a) $t=120$, (b) $t=200$, showing the gradual convergence to the spatially periodic target.

ond example, we explore the viability of controlling a turbulent state into another one. In both cases, we apply the global pinning control

$$\mathbf{f}(\mathbf{u},\mathbf{u}_t)=\epsilon(\mathbf{u}-\mathbf{u}_t) \tag{5}$$

to the right-hand side of Eq. (1), with $\mathbf{u}_t=(u_t,v_t)$ being the time-varying velocity fields of the target, e.g., Eq. (4), and $\epsilon<0$ being the coupling strength. The control is not added until Eq. (1) has been integrated to $t=100$, ensuring that the system has passed the transient stage and is in the turbulent regime. Figures 1(a) and 1(b) depict two turbulent vorticity fields $\omega(x,y,t)=v_x-u_y$ at $t=100$ and $t=250$, respectively. It is observed that the turbulent state gradually converges to the target after the control mechanism is switched on. The vorticity contour plots of the controlled flow are shown in Fig. 2. Obviously, the turbulent state has been successfully controlled into the spatially periodic target state (4). The convergence to the target under different coupling strength is shown in Fig. 4(a). Similar control results have been observed when the pinning coupling is turned on at both an earlier time ($t=60$) and a later time ($t=200$). Moreover, we also use the stationary pattern

$$\begin{aligned} u_t(x,y,t)&=-\ \gamma\cos(kx)\sin(ky),\\ v_t(x,y,t)&=\gamma\ \sin(kx)\cos(ky), \end{aligned} \tag{6}$$

as the target. Once again the control of the turbulent state to the target is successful.

We next consider the control of an arbitrary turbulent state shown in Fig. 1(b), to a target turbulent dynamics

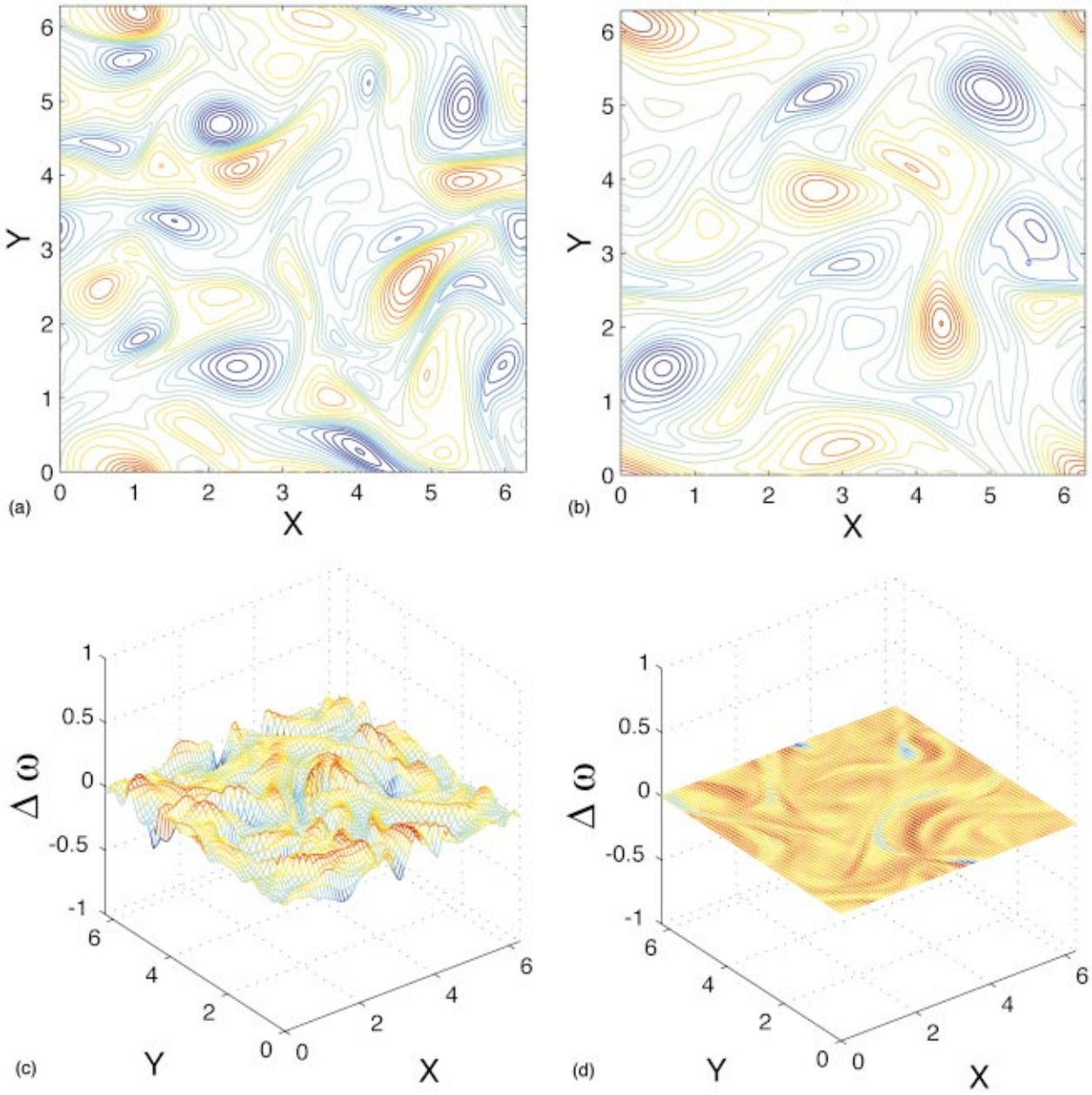

FIG. 3. (Color) (a),(b) Contour plots of the vorticity field of turbulent target at (a) $t=100$, (b) $t=250$, respectively; (c),(d) the difference of the vorticity fields between the target and the response system at (c) $t=120$, (d) $t=200$, respectively; showing the gradual convergence of the controlled system to the turbulent target.

shown in Fig. 3(b). The turbulent target is generated by using Eq. (3) with $k_0=3.0$ as initial energy spectrum. The time evolution of both the target system and the response system is governed by the Navier–Stokes equations, Eq. (1), while the response system is unidirectionally coupled to the target system by the coupling (5). We observe that the state of the response system gradually converges to the turbulent state of the target as shown in Figs. 3(c) and 3(d). The convergence under different coupling strength is shown in Fig. 4(b). It is noted that the control of chaos using unidirectional coupling is equivalent with the synchronization of two systems. Therefore, this control of turbulence can also be understood in terms of synchronization of two turbulent dynamics.

The effectiveness of the present control process remains to be studied. Mathematically, the control of a spatiotemporal dynamics to a target one implies

$$\lim_{t\to\infty}\|\Delta\omega(x,y,t)\|\to 0, \tag{7}$$

where $\Delta\omega(x,y,t)=\omega(x,y,t)-\omega_t(x,y,t)$. The effectiveness of the control can be measured by defining the variance

$$\sigma(t)=\left\{\frac{1}{N_xN_y}\sum_{i=1,j=1}^{N_x,N_y}[\Delta\omega(i,j,t)]^2\right\}^{1/2}. \tag{8}$$

Figures 4(a) and 4(b) plot the variance versus time for various coupling strengths for the two control cases discussed above. We studied the convergence of the variance with re-

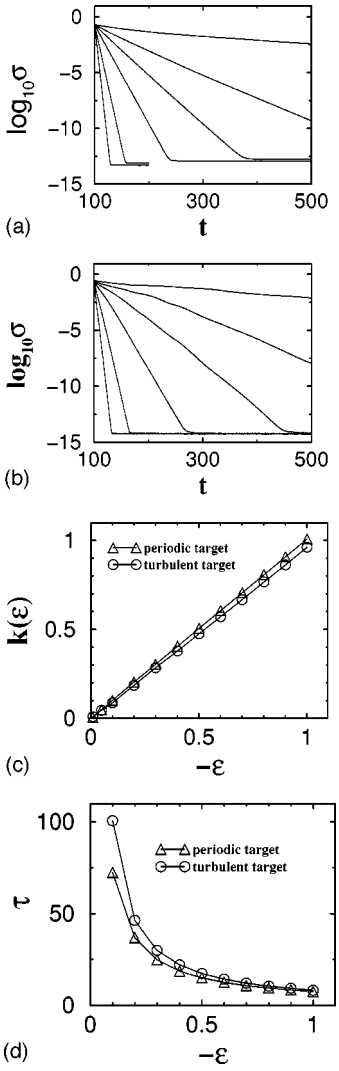

FIG. 4. Characterization of turbulence control. (a), (b) The variance versus time for approaching the time-varying periodic target (a), and the turbulent target (b), respectively; from top to bottom: $\epsilon=-0.01,-0.05,-0.1,-0.2,-0.5,-1.0$; (c) the linear scale between $k(\epsilon)$ and ϵ; (d) the transient time (the variance is truncated at 10^{-4}) versus the coupling strength.

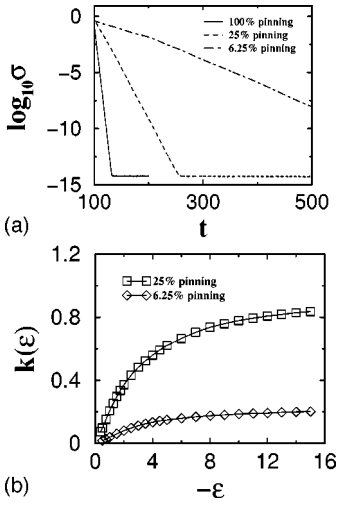

FIG. 5. Turbulent control by using the local pinning strategy. (a) The same as Fig. 4(b) ($\epsilon=-1.0$); (b) the linear scale between $k(\epsilon)$ and ϵ breaks down.

spect to the coupling strength in a large range from $\epsilon=-0.01$ to -10, and found that approximately the variance decays exponentially

$$\sigma(t)\propto e^{-k(\epsilon)t}, \tag{9}$$

even for a very small coupling strength, see Figs. 4(a) and 4(b).

Qualitatively, $k(\epsilon)$ can be understood as the convergence speed and thus can be used to characterize the effectiveness of control. By extensive numerical experiments, we further find that $k(\epsilon)$ has a simple linear relation with respect to the coupling strength, i.e.,

$$k(\epsilon)=-\alpha\epsilon \quad (\epsilon<0) \tag{10}$$

over a wide range of parameters studied. It is interesting to note that α is almost the same in two different examples as shown in Fig. 4(c), where the two straight lines approximately have the slopes $\alpha=1.01$ and 0.963, respectively. The exponential form in Eq. (9) indicates that the convergence to the target state is entirely driven by the coupling scheme. In other words, the dynamics of the response system, after the initial period, is dominated by the coupling term, which admits an exponential decay solution. Since the coupling term scales linear to the coupling strength ϵ, the linear scaling law is found.

We define the transient time τ as the time for the response system to converge to the target and it is proportional to $(\alpha|\epsilon|)^{-1}$. Obviously, the transient time will be relatively long for the case of a weak coupling. The transient time as a function of the coupling strength is plotted in Fig. 4(d). For a typical value of $\epsilon=-0.5$, the transient time is of the order of 10. It decays rapidly with respect to the increase of the coupling strength.

The feature of the above global pinning control strategy is that it needs to couple all the corresponding sites between the target and the response system. In other words, the number of the controllers involved equals to the dimension of the system. For some low-dimensional dynamical systems, such as maps or ordinary partial differential equations, it can be experimentally realized. However, physically it is difficult to apply the pinning control to the continuous systems, e.g., systems described by the partial differential equations. To overcome this difficulty, the local pinning coupling as an important step towards realistic control of spatiotemporal chaos has been proposed.[7] For the current study of control of flow turbulence, it remains to verify whether the same can be achieved by using a local pinning control. To this end, we test two local pinning schemes, in which a fourth (25%) and a sixteenth (6.25%) of the original pinning sites are kept and evenly distributed. The turbulent target is considered and the result of control is given in Fig. 5. Obviously, the local pinning control is also very successful for the controlling of flow turbulence governed by two-dimensional Navier–

Stokes equations. It is found that even using local coupling, as long as the coupling strength is sufficiently large, the exponential convergence between the turbulence under control and the target still approximately holds. However, the linear scaling law between the exponential rate $k(\epsilon)$ and coupling strength ϵ found in the previous cases breaks down. Such a break down is due to the local pinning control strategy. Note that new curve is always below the line of the linear scaling law, which indicates that the local pinning scheme is not as efficient as the global one. Since only partial sites of the response system are coupled to the driven system, the influence of the driven state cannot be ''felt'' immediately by all sites of the response system. Such a time delay leads to the reduction of the original linear scaling law to the curve which is underneath the linear scaling line.

IV. WAVELET CHARACTERIZATION

Turbulence inherently involves a wide range of spatial scales. The various spatial modes interact through the nonlinear convective term in Navier–Stokes equations, leading to energy transfer among different scales. Due to this multiscale nature of turbulence, wavelets and wavelet packets provide a powerful mathematical tool for modeling, analyzing, and computing turbulence.[14] In the present work, a recently proposed wavelet method is utilized to characterize the turbulence field. Compared with the traditional method, i.e., the Fourier transform, the present wavelet method has the advantage of providing multiscale information. Unlike the usual application of wavelet analysis to turbulence, the present wavelet approach provides ''time evolution histories'' for different scale components. The detailed description of the approach is given in Ref. 15. A schematic plot of the three-scale wavelet sub-band decomposition is given in Fig. 6(a). Here H denotes the high frequency (small scale) while L denotes the low frequency (large scale). The subscript number denotes the scale of the wavelet decomposition. Daubechies-8 wavelets are employed.

Figure 6(b) characterizes the temporal evolution and convergence of two turbulent dynamics in terms of wavelet sub-band energies $\rho_m^{HH}(t)$ $(m=1,2,3)$, corresponding to the three high-frequency sub-bands HH_m $(m=1,2,3)$ shown in Fig. 6(a), respectively. It is found that during the first evolution stage $(t<70)$, there is a significant increase of the turbulent energy at three small scales. This may correspond to the generation of small-scale structures, e.g., vorticity-gradient sheets, from the relatively smooth initial velocity fields. After this stage, the turbulence becomes fully developed as indicated by vanishing of the vorticity-gradient sheets and the self-organization, advection and merger of the coherent vortices (see Figs. 1 and 3). Accordingly, the energies at all three high-frequency sub-bands decrease. After turning on the control at $t=100$, the turbulence sub-band energies of the response system gradually converge to those of the target as shown in Fig. 6(b), symbolizing the success of the pinning control strategy.

It is well known that the long-term evolution of freely decaying two-dimensional turbulence is characterized by the advection and coalesce of the coherent vortices as well as the formation of large scale vortices such as stable dipoles. Figures 6(c) and 6(d) show the energy evolution and transfer among different spatial scales during this dynamical process. An inverse energy transfer (from small towards large scales)[10] can be effectively characterized by the current wavelet method. It is seen that during the initial transient period, the energies at all three small scales increase, while

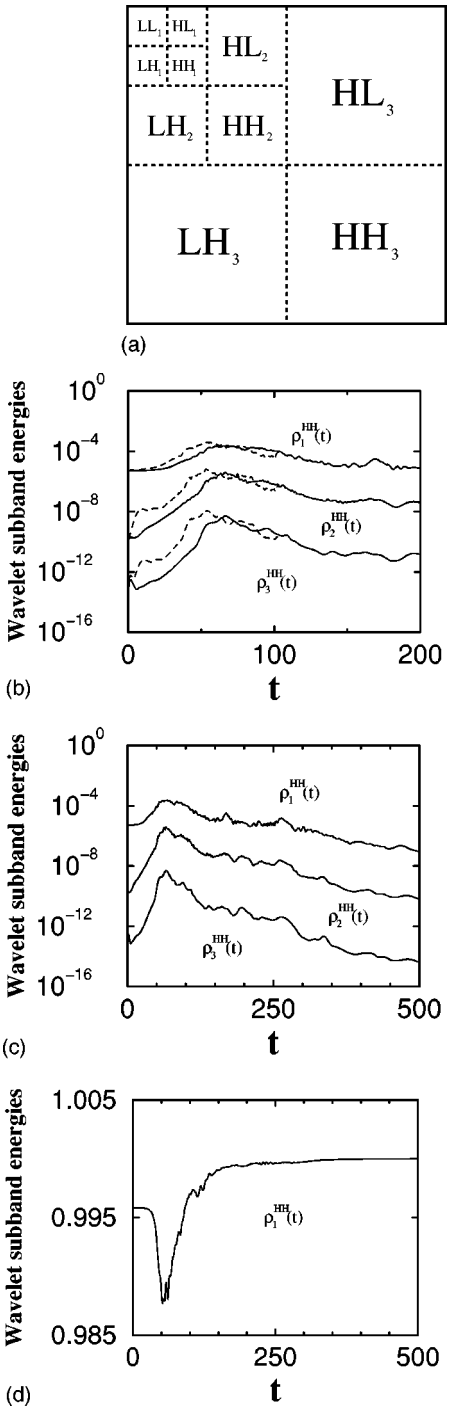

FIG. 6. Wavelet multiscale characterization of turbulence control ($\epsilon = -1.0$). (a) A schematic plot of wavelet sub-band decomposition; (b)–(d) the evolution of wavelet sub-band energies. (b) the early evolution of the target system (solid lines) and the response system (dashed lines); (c),(d) the evolution of the target system in small scale sub-bands (c) and the large scale one (d).

the energy at the large scale decrease. When the turbulence becomes fully developed, the energies at all three small scales decay with time. Although this decay is not monotonic, its trend is obvious. The reason of the non-monotonic decay is that the vorticity filaments generated during the merger of vortices are highly oscillatory. On the contrary, the wavelet sub-band energy $\rho_1^{LL}(t)$, which corresponds to the large scale LL_1 shown in Fig. 6(a), increases during the time evolution, as shown in Fig. 6(d). Physically, the energy transfer towards large scales corresponds to the organization and merger of coherent vortices in freely decaying two-dimensional turbulence. Therefore, the dynamics of two-dimensional turbulence is dominated by the coherent vortices, which is essentially different form the traditional picture of three-dimensional turbulence as a chaotic velocity field.

V. CONCLUDING REMARKS

In summary, we have studied the utility and effectiveness of techniques developed for low-dimensional chaotic systems for controlling flow turbulence governed by the Navier–Stokes equations. By using both global pinning and local pinning strategies, we show that the turbulent flow can be controlled to desired target states, including the time-varying analytical solution of the Navier–Stokes equations and an evolving turbulent state. In both cases, the dynamics of the response system converges to the time-varying target exponentially. A linear scaling between the exponential rate and the coupling strength is observed for the global pinning control within the parameter range of small and moderate coupling strength. However, such a linear scaling law breaks down when the local pinning control is employed. The effectiveness of the control scheme is also confirmed by examining the transient time required for the response system to convert to the target state. A newly developed wavelet multiscale technique is utilized to characterize the present control of turbulence.

Undoubtedly, turbulence control has been one of the central issues in modern science and engineering. As pointed out by Gad-el-Hak (in Ref. 2, p. 117), ''future systems for control of turbulent flows in general and turbulent boundary layers in particular could greatly benefit from the emerging of the science of chaos control, ...'' Indeed, the concepts and the diverse strategies arising from the extensive study of chaos control in the last decade has shed light on the control of flow turbulence. The findings in the present work verify the feasibility of such a control.

However, the practical realization of flow control turns out to be a difficult and complicated task from engineering perspective. In the past several decades, there is much empirical exploration on passive control methods using polymers and riblets.[2] The control schemes used in the present study is an active control strategy and it requires that the controlled variable be measured, fed back and compared with a reference target. Practically, the successful implementation of this control strategy lies in how to interact with the flow. For example, one must have a series of properly disposed sensors to detect the status of the turbulence, and actuators to produce the desired flow perturbations. In the past, direct flow manipulation was very difficult, but is now expected to become possible with microsensors and microactuators of micron size fabricated by micro-electro-mechanical-systems (MEMS) technology. Moreover, these miniature transducers can be integrated to complete the feedback control loop of sensing, information processing and actuation. Although the control strategy proposed in this paper can be implemented with modern technology, there is a long way toward the mature stage of controlling flow turbulence.

[1] A concise and authoritative review with a good number of cross references on fluid turbulence: K. R. Sreenivasan, Rev. Mod. Phys. **71**, S383 (1999).
[2] The engineering aspects of controlling turbulence are described by M. Gad-el-Hak, in *Flow Control: Fundamentals and Practices*, edited by M. Gad-el-Hak, A. Pollard, and J.-P. Bonnet (Springer-Verlag, New York, 1998).
[3] B. A. Huberman and E. Lumer, IEEE Trans. Circuits Syst. **37**, 547 (1990); E. A. Jackson and A. Hubler, Physica D **44**, 407 (1990); R. Lima and M. Pettini, Phys. Rev. A **41**, 726 (1990); Y. Braiman and I. Goldhirsch, Phys. Rev. Lett. **66**, 2545 (1991); V. Petrov, V. Gaspar, J. Masere, and K. Showalter, Nature (London) **361**, 240 (1993); G. Hu and Z. Qu, Phys. Rev. Lett. **72**, 68 (1994); D. Auerbach, *ibid.* **72**, 1184 (1994); I. Aranson, H. Levine, and L. Tsimring, *ibid.* **72**, 2561 (1994); G. A. Johnson, M. Löcher, and E. R. Hunt, Phys. Rev. E **51**, R1625 (1995); L. Kocarev, U. Parlitz, T. Stojanovski, and P. Janjic, *ibid.* **56**, 1238 (1997); a review on theory and experiments of controlling chaos: S. Boccaletti, C. Grebogi, Y.-C. Lai, H. Mancini, and D. Maza, Phys. Rep. **329**, 103 (2000).
[4] E. Ott, C. Grebogi, and J. A. Yorke, Phys. Rev. Lett. **64**, 1196 (1990).
[5] J. Lumley and P. Blossey, Annu. Rev. Fluid Mech. **30**, 311 (1998).
[6] K. Pyragas, Phys. Lett. A **170**, 421 (1992).
[7] J. Xiao, G. Hu, J. Yang, and J. Gao, Phys. Rev. Lett. **81**, 5552 (1998); S. Boccaletti, J. Bragard, and F. T. Arecchi, Phys. Rev. E **59**, 6574 (1999); L. Junge and U. Parlitz, *ibid.* **61**, 3736 (2000).
[8] G. W. Wei, Phys. Rev. Lett. **86**, 3542 (2001); B. S. V. Patnaik and G. W. Wei, *ibid.* **88**, 054502 (2002); J. R. Minkel, Phys. Rev. Focus January 28, 2002.
[9] In 2D turbulence, the pseudoscalar vorticity $\omega=(0,0,\omega)$ is perpendicular to the velocity gradients. Therefore the vorticity is Lagrangian invariant of the flow in the limit of small viscosities and the mechanism of vortex stretching is forbidden.
[10] R. H. Kraichnan and D. Montgomery, Rep. Prog. Phys. **43**, 547 (1980); U. Frisch, *Turbulence* (Cambridge University Press, Cambridge, 1995).
[11] In 3D turbulence, the energy transfer from large scales to small scales through vortex stretching. Contrarily, in the 2D case, the nonlinear interaction leads to an inverse energy cascade and a direct enstrophy cascade due to the dual conservation of energy and enstrophy. Experiments on quasi-2D turbulence were reported by J. Sommeria, J. Fluid Mech. **170**, 139 (1986); P. Tabeling, S. Burkhart, O. Cardoso, and H. Willaime, Phys. Rev. Lett. **67**, 3772 (1991).
[12] S. Y. Yang, Y. C. Zhou, and G. W. Wei, Comput. Phys. Commun. **143**, 113 (2002).
[13] P. Santangelo, R. Benzi, and B. Legras, Phys. Fluids A **1**, 1027 (1989); P. Orlandi, *Fluid Flow Phenomena, A Numerical Toolkit* (Kluwer Academic, Dordrecht, 2000).
[14] M. Farge, N. Kevlahan, V. Perrier, and K. Schneider, in *Wavelets and Physics*, edited by J. C. van den Berg (Cambridge University Press, Cambridge, 1999).
[15] S. Guan, C.-H. Lai, and G. W. Wei, Physica D **163**, 49 (2002).